Solar Forcing of Electron and Ion Auroral Inputs

Barbara A. Emery (NCAR), Ian G. Richardson (GSFC), David S. Evans (NOAA), Frederick J. Rich (LL/MIT), Gordon Wilson (AFRL), Sarah Gibson (NCAR), Giuliana deToma (NCAR), Terry Onsager (NOAA), and Jiuhou Lei (U CO)

HEPPA Oct 2009, Boulder

ABSTRACT

We assess the contribution of solar forcing from the interplanetary magnetic field (IMF) |B| and solar wind velocity (Vsw) on the auroral inputs from intercalibrated NOAA and DMSP satellite-track in-situ particle measurements. Periodicities in Vsw and the global electron (Pe) and ion power (Pi) are calculated using Lomb-Scargle (L-S) and wavelet analyses. We examine two different solar minimum periods in a broader context, including radiation belt electrons >2 MeV. The first Whole Sun Month (WSM) interval (96223-96252) had a strong solar magnetic dipole. Strong 'semiannual' equinoctial periodicities of ~20% variation in Vsw and 40% variation in Pe were found. In the present solar minimum, the solar magnetic field is weaker with larger quadrupole components during the Whole Heliospheric Interval (WHI, 08080-08107). Strong 9-d amplitudes of ~30% variation in Vsw and ~40% variation in Pe and Pi were found. This 9-d periodicity was also found in the IMF |B|, in the CHAMP neutral density at 400 km, and in the outer radiation belt electrons >2 MeV. Solar periodicities are also examined using the available parameters during previous solar minima in 1985-1986 and in 1975-1976.

Estimates of the electron hemispheric power (HPe) into the auroral regions from particle detectors on NOAA and DMSP satellites were inter-calibrated over 31 years and 24 satellites.

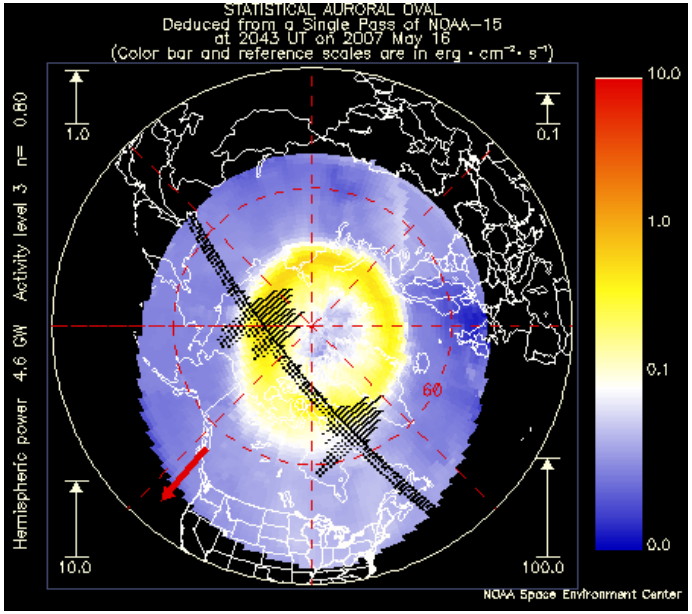

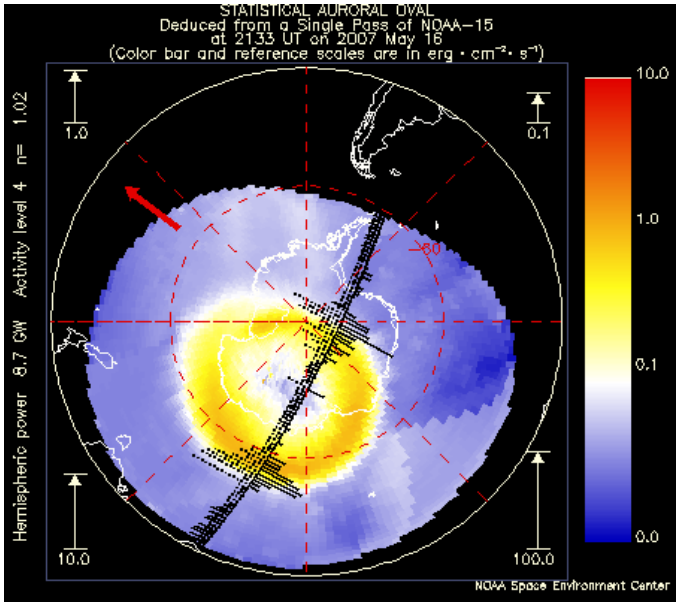

The electron hemispheric power (HPe) is found in both hemispheres on an hourly basis. The sum of the Northern and Southern hemispheres is the auroral electron power (Pe).

Uncalibrated HPe

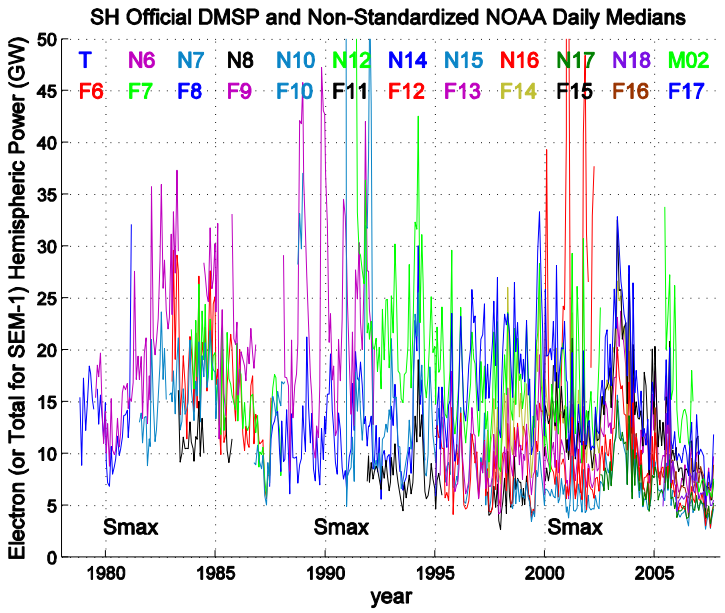

Calibrated HPe

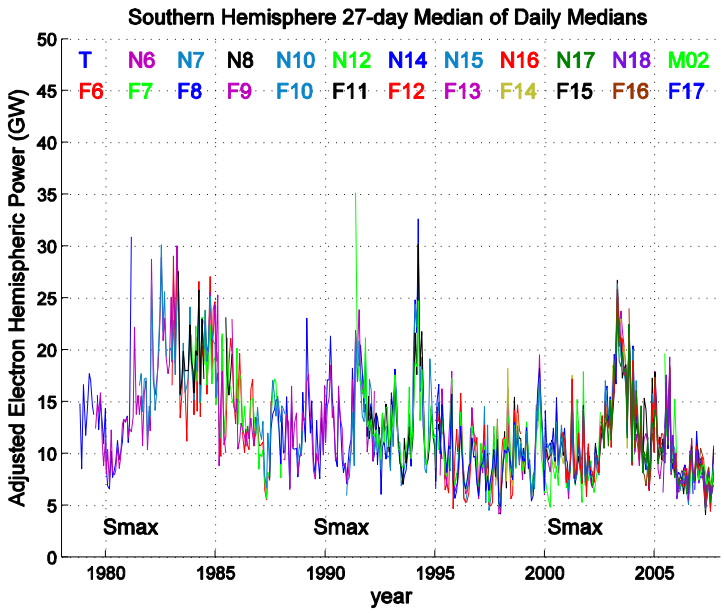

The ion hemispheric power (HPi) is found from 5 NOAA SEM-2 satellites as HPi=Hpt-Hpe (<20keV)

Arrows show high voltage gain increases for N16. Baseline is set to N12 or ~2x too high.

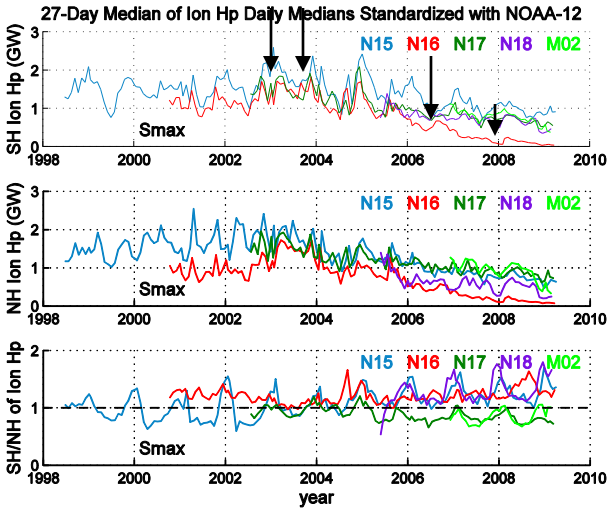

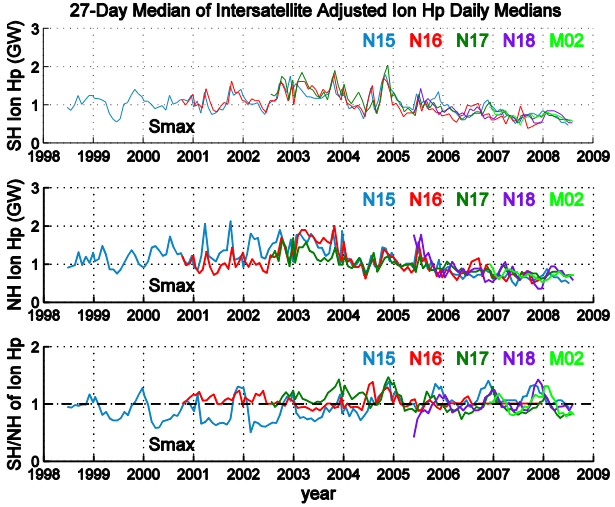

old

new

'real' values; baseline increased to agree with DMSP ions <20 keV

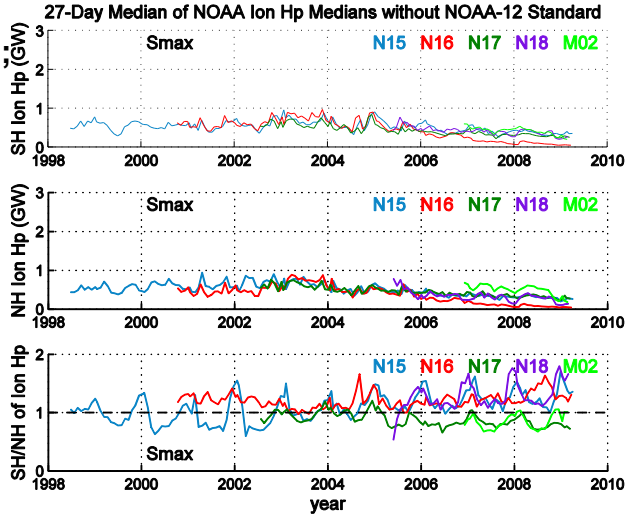

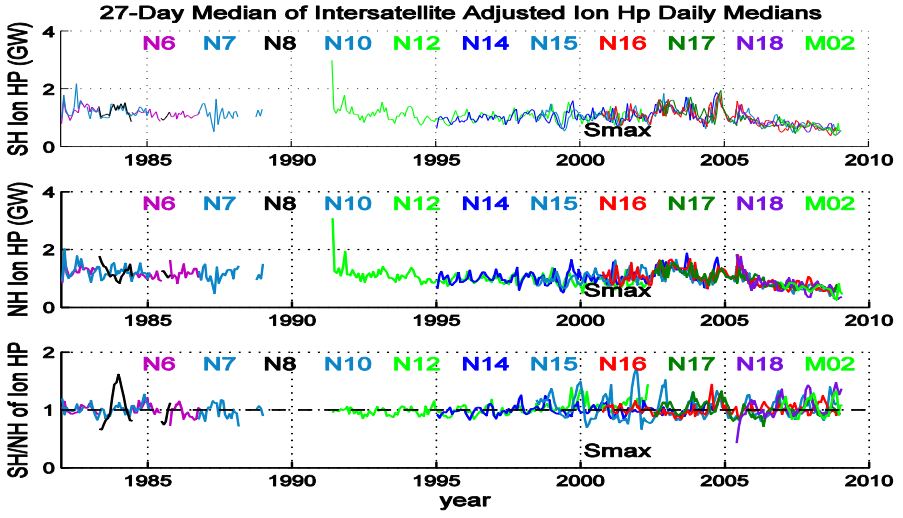

Contributions of Solar Wind Structures to Auroral Power

Average hourly Vsw attributed to solar wind structure as 27-day averages

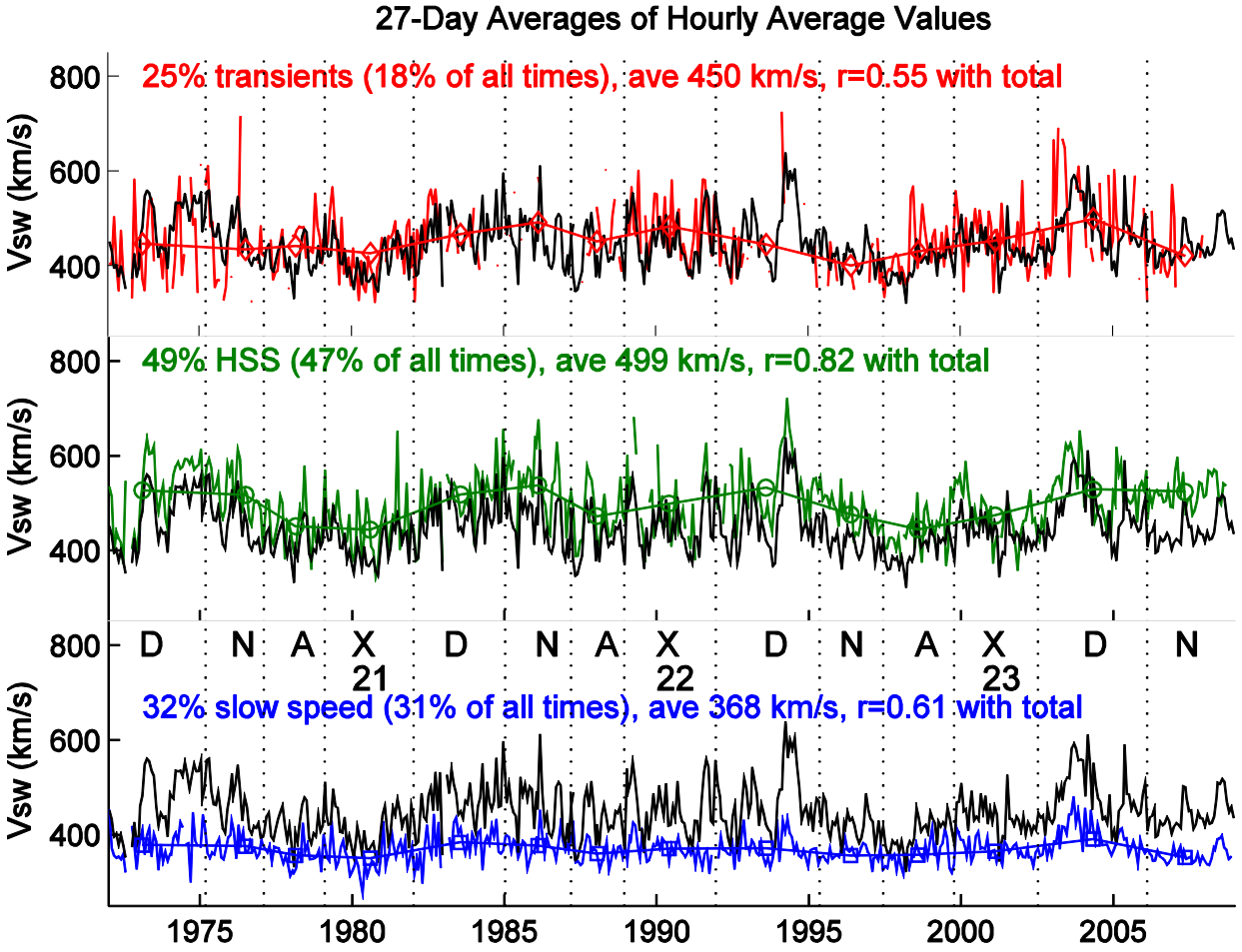

Average hourly IMF attributed to solar wind structure as 27-day averages

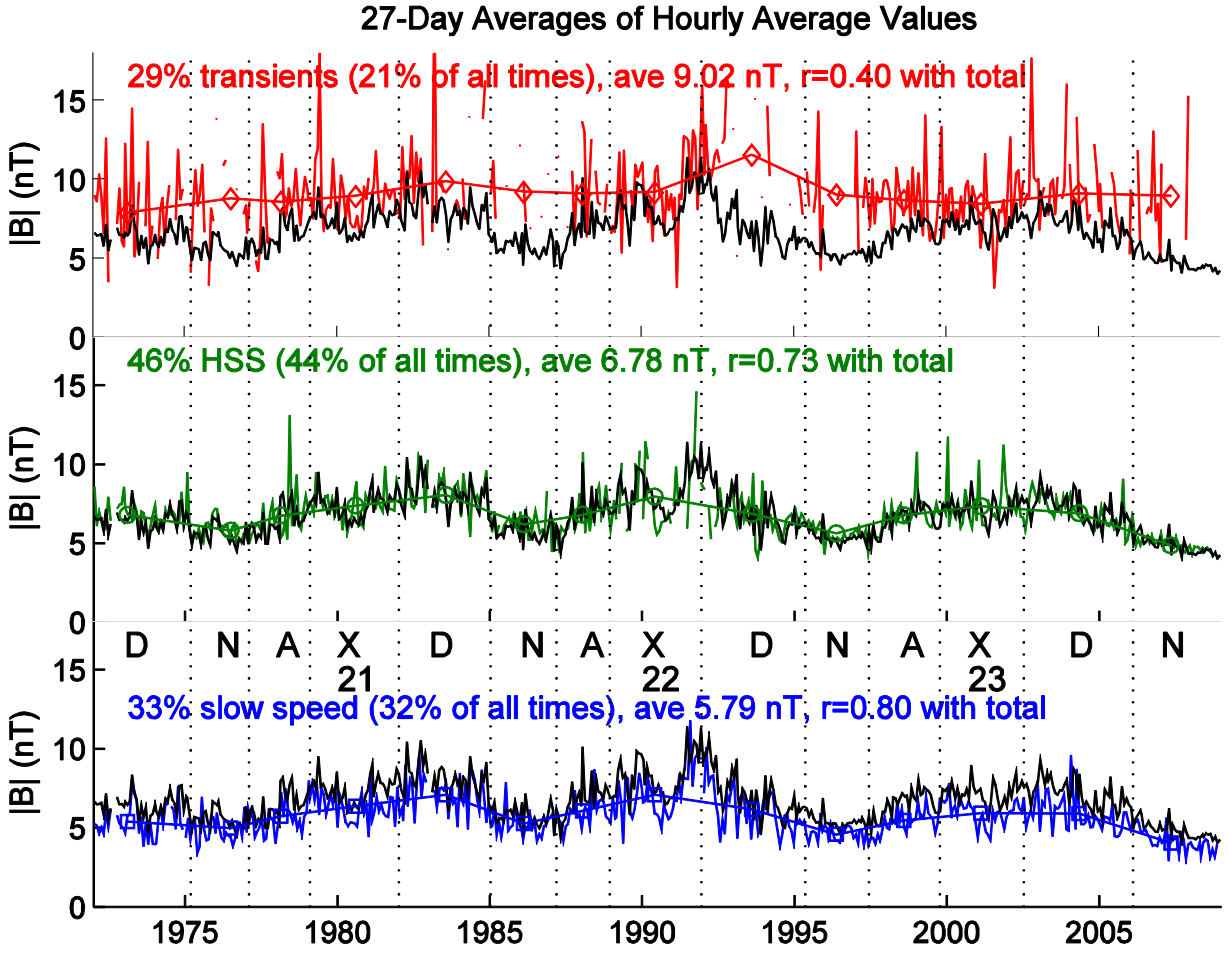

Average hourly Pe attributed to solar wind structure as 27-day averages

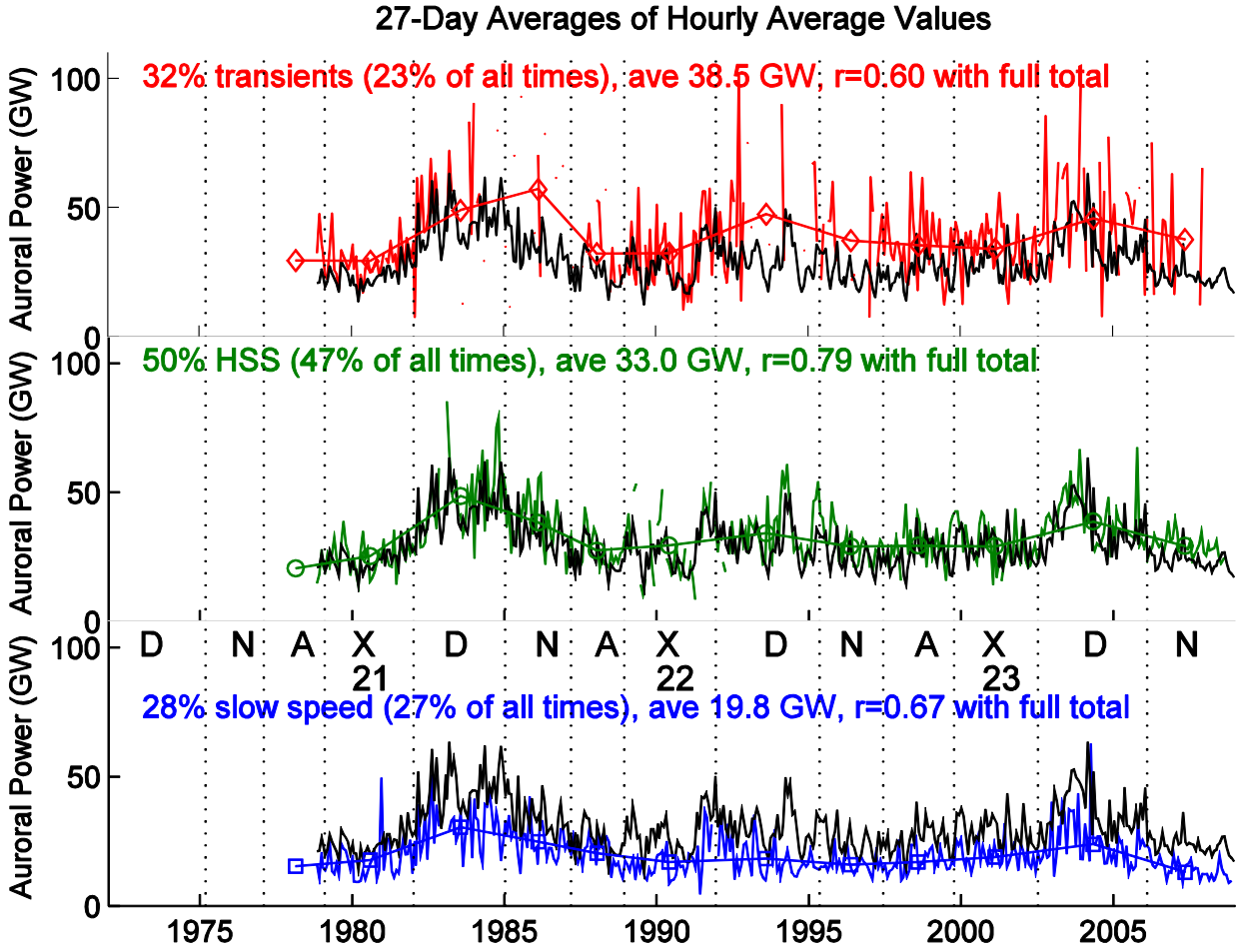

Correlation of Pe with Vsw|B|

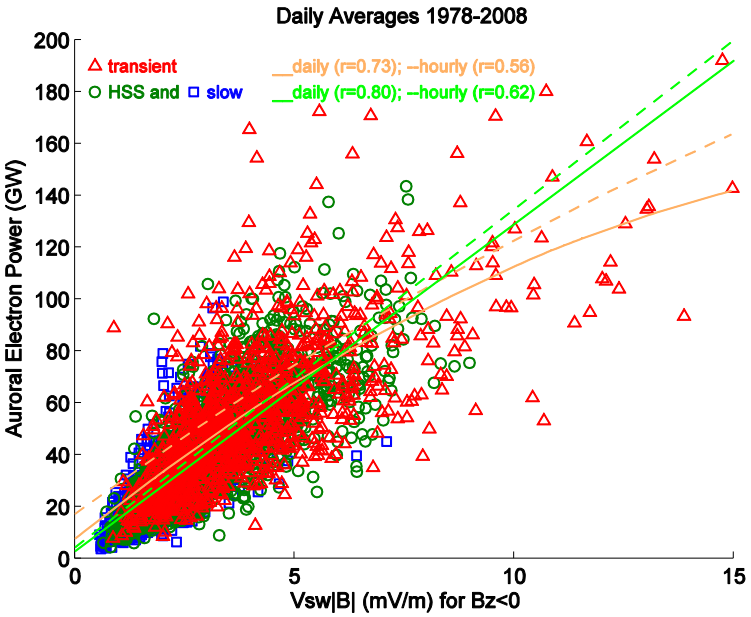

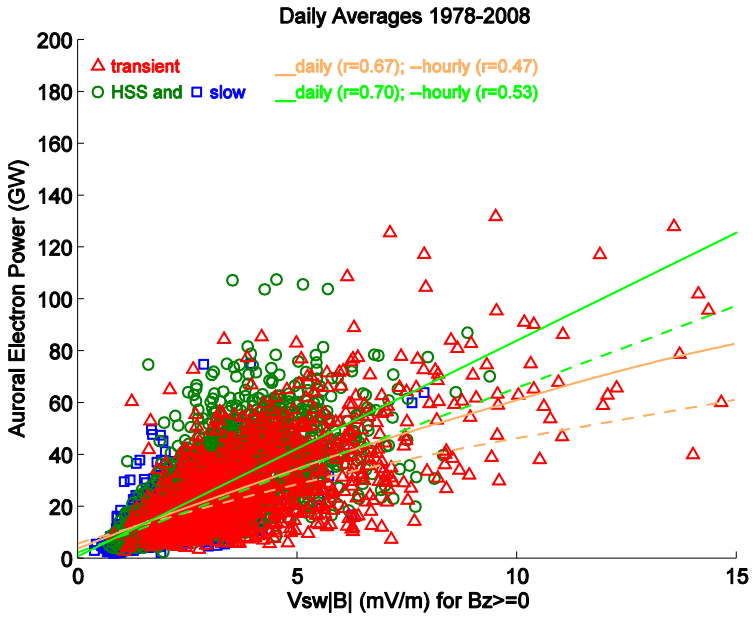

Transient fit higher than HSS+slow for Bz<0, lower for Bz>0, so an increase in |B| (or Bz) is more,less effective for Bz<0,>0.

Solar Rotational Periodicities in the total Vsw, Pe, and Pi

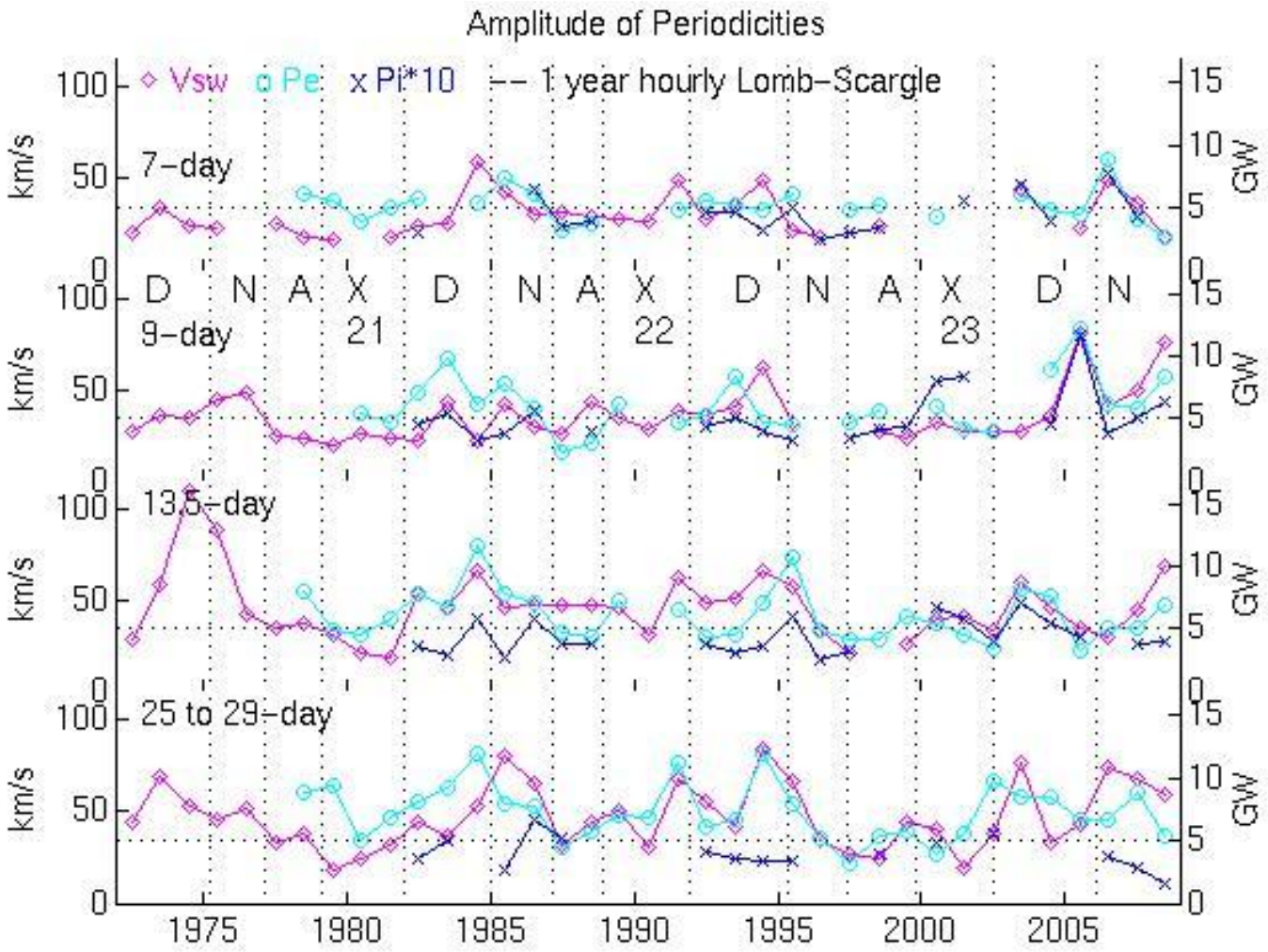

Largest amplitudes in Descending (D) and Minimum (N) phases of the solar cycle.

Two Solar Minimum Comparisons

1996 WSM and 2008 WHI Minima

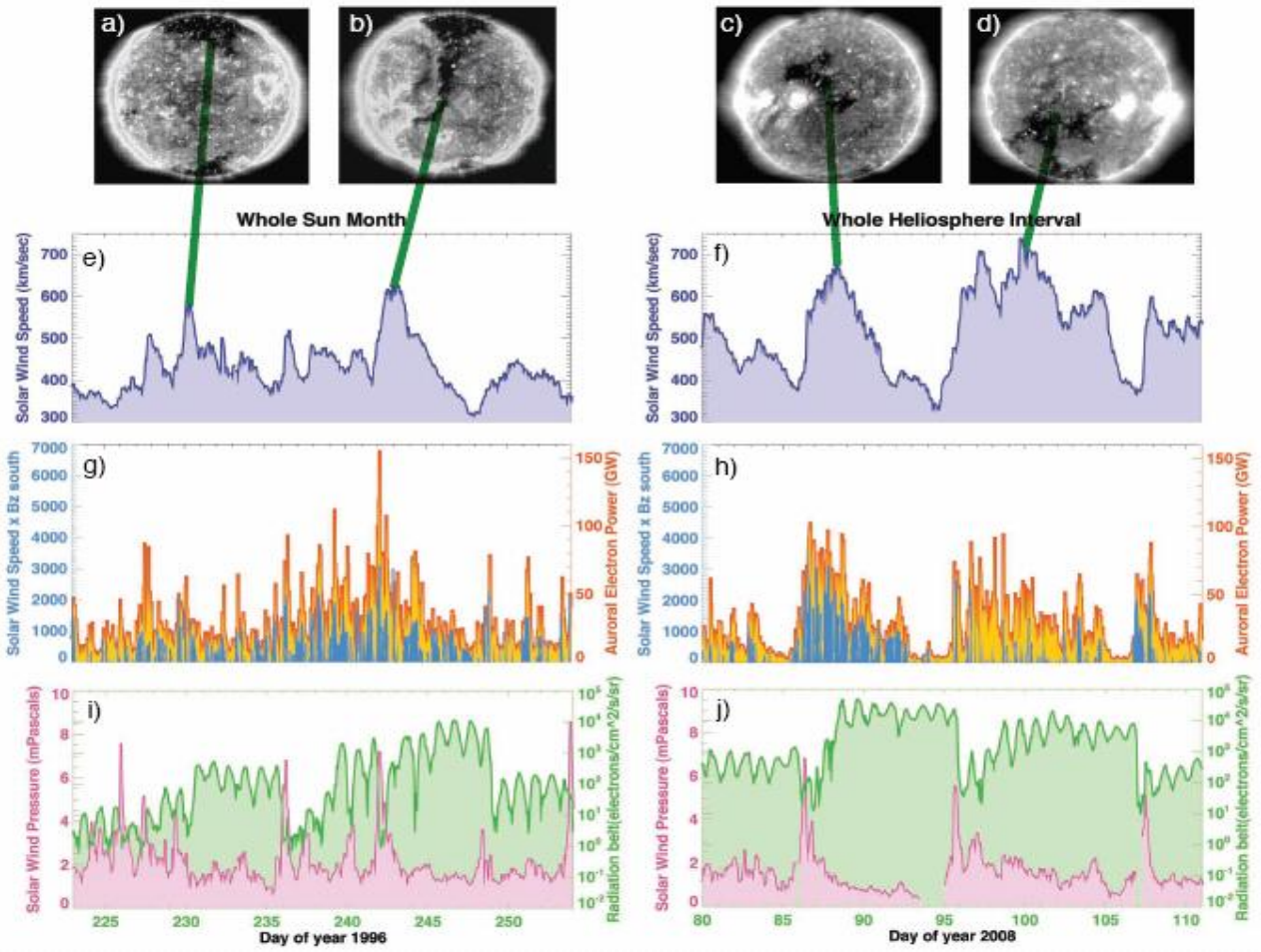

SOHO/EIT images (a-d) show coronal holes as dark regions in extreme-ultraviolet emission. Radiation belt electrons >2 MeV (i-j) initially decrease with pressure pulses at the leading edges of HSS, and then are high until the next leading edge pressure pulse. [Gibson et al., JGR, 2009]

WSM and WHI in Context

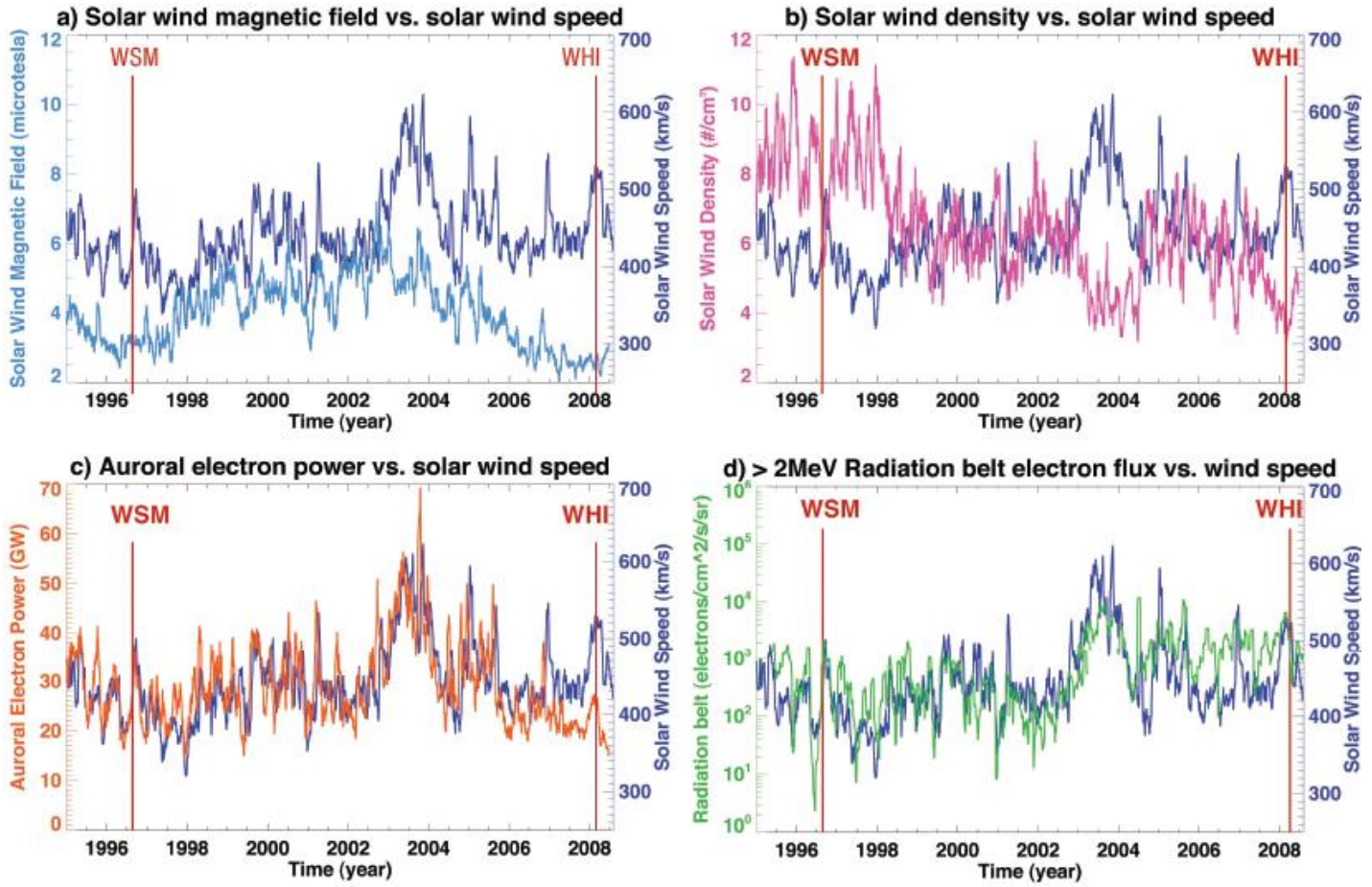

Vsw in dark blue shows an increase of ~8% from WSM to WHI. The sunspot cycle is similar to the solar wind B field in (a), and decreases ~15% between WSM and WHI. The solar wind density (Dsw) in (b) shows a stronger decrease of ~35%. Pe in (c) is nearly coincident with Vsw except it decreases ~5% from WSM to WHI because of the decrease in B. The radiation belt electrons in (d) increases, possibly because of lower loss rates (Dsw less).

Magnetic field (-15%) & Solar wind speed (+8%)

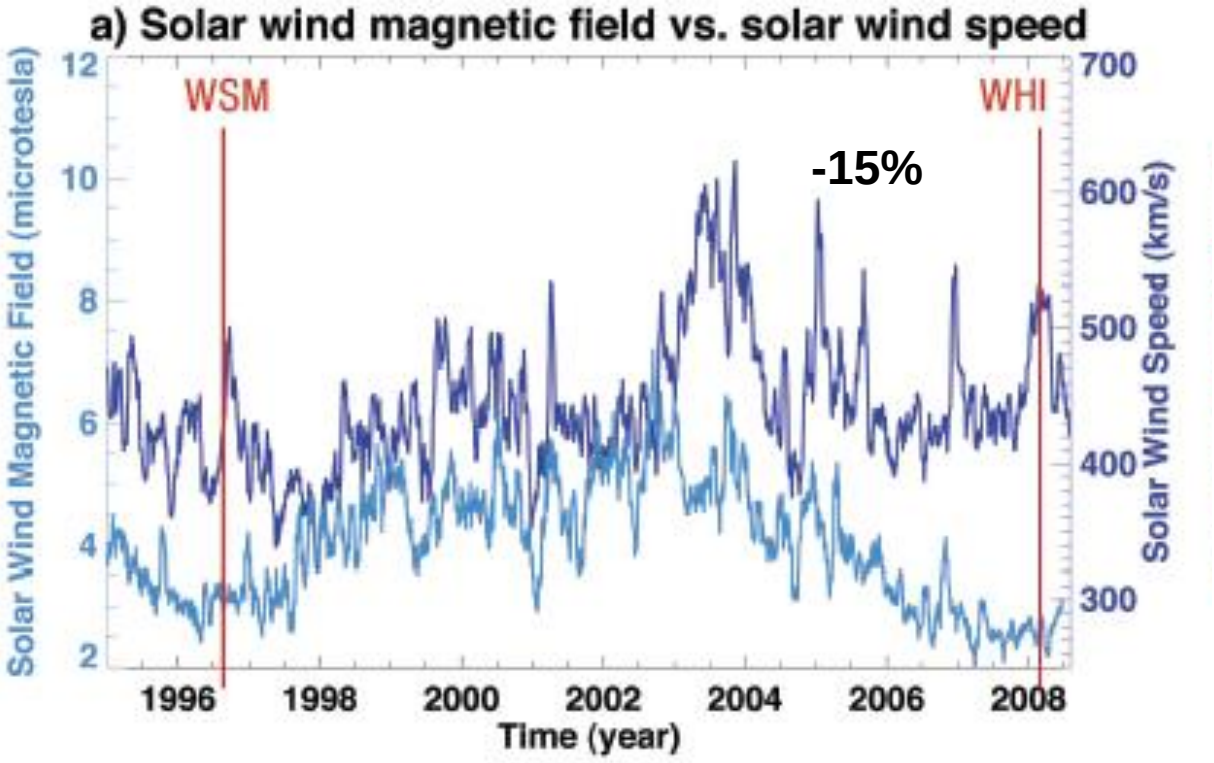

Vsw in dark blue shows an increase of ~8% from WSM to WHI. The sunspot cycle is similar to the solar wind B field in (a), and decreases ~15% between WSM and WHI. The solar wind density (Dsw) in (b) shows a stronger decrease of ~35%. Pe in (c) is nearly coincident with Vsw except it decreases ~5% from WSM to WHI because of the decrease in B. The radiation belt electrons in (d) increases, possibly because of lower loss rates (Dsw less).

Solar wind density (-35%) & Solar wind speed (+8%)

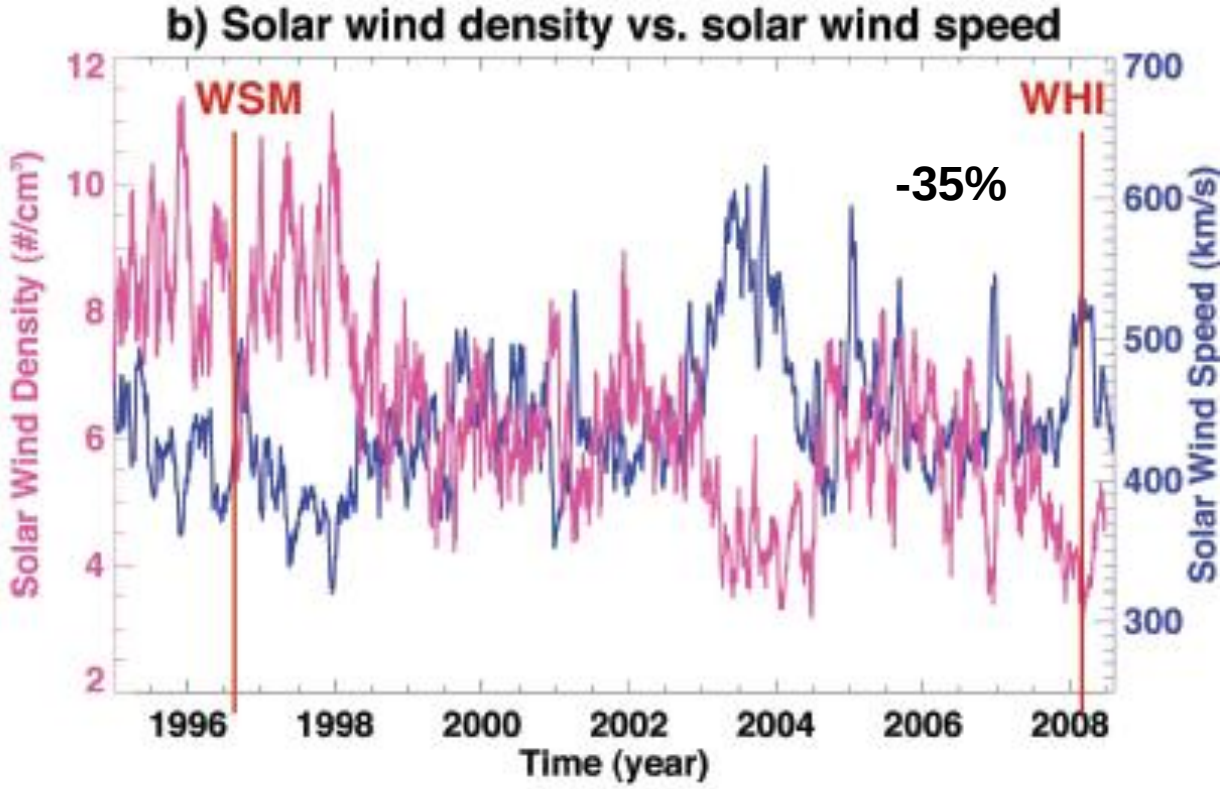

Vsw in dark blue shows an increase of ~8% from WSM to WHI. The sunspot cycle is similar to the solar wind B field in (a), and decreases ~15% between WSM and WHI. The solar wind density (Dsw) in (b) shows a stronger decrease of ~35%. Pe in (c) is nearly coincident with Vsw except it decreases ~5% from WSM to WHI because of the decrease in B. The radiation belt electrons in (d) increases, possibly because of lower loss rates (Dsw less).

Auroral Power (-5%) & Solar wind speed (+8%)

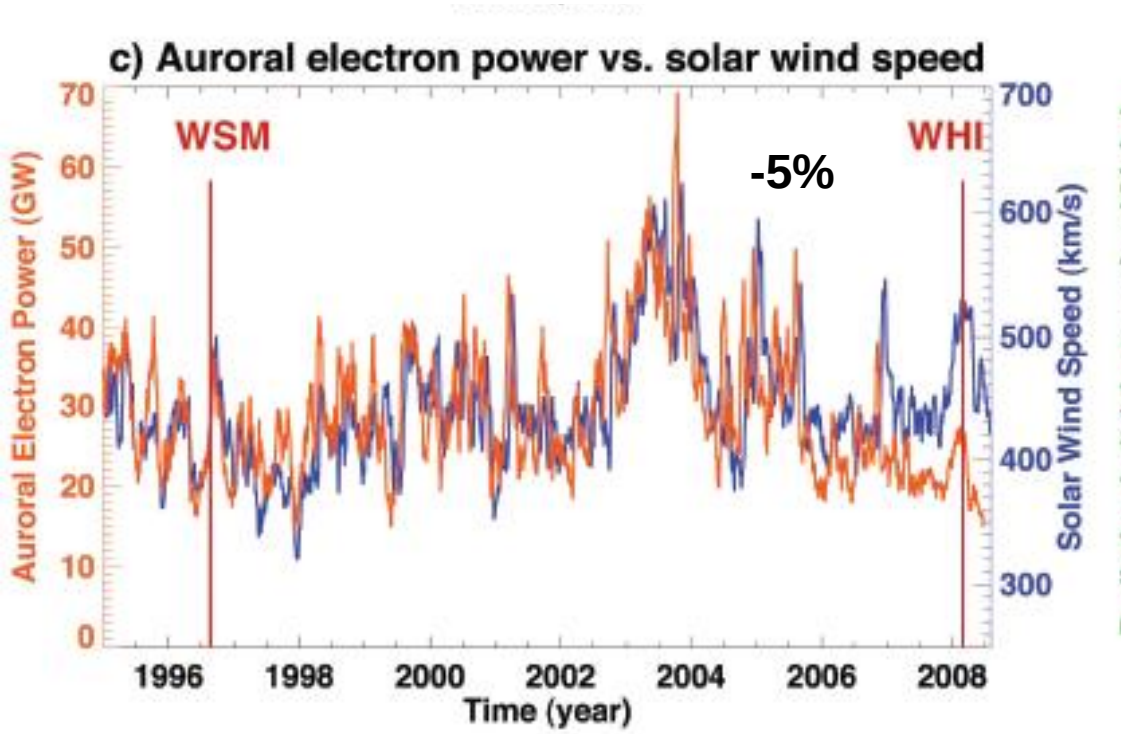

Vsw in dark blue shows an increase of ~8% from WSM to WHI. The sunspot cycle is similar to the solar wind B field in (a), and decreases ~15% between WSM and WHI. The solar wind density (Dsw) in (b) shows a stronger decrease of ~35%. Pe in (c) is nearly coincident with Vsw except it decreases ~5% from WSM to WHI because of the decrease in B. The radiation belt electrons in (d) increases, possibly because of lower loss rates (Dsw less).

Radiation belt (x3.4) & Solar wind speed (+8%)

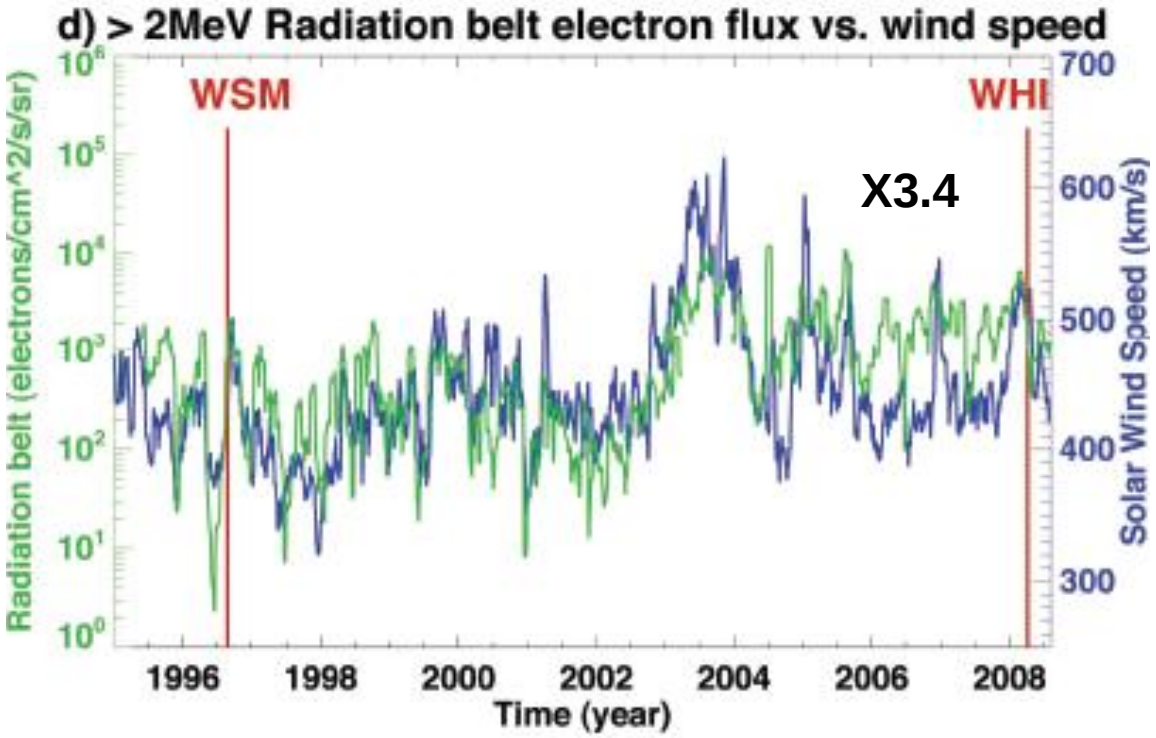

Vsw in dark blue shows an increase of ~8% from WSM to WHI. The sunspot cycle is similar to the solar wind B field in (a), and decreases ~15% between WSM and WHI. The solar wind density (Dsw) in (b) shows a stronger decrease of ~35%. Pe in (c) is nearly coincident with Vsw except it decreases ~5% from WSM to WHI because of the decrease in B. The radiation belt electrons in (d) increases, possibly because of lower loss rates (Dsw less).

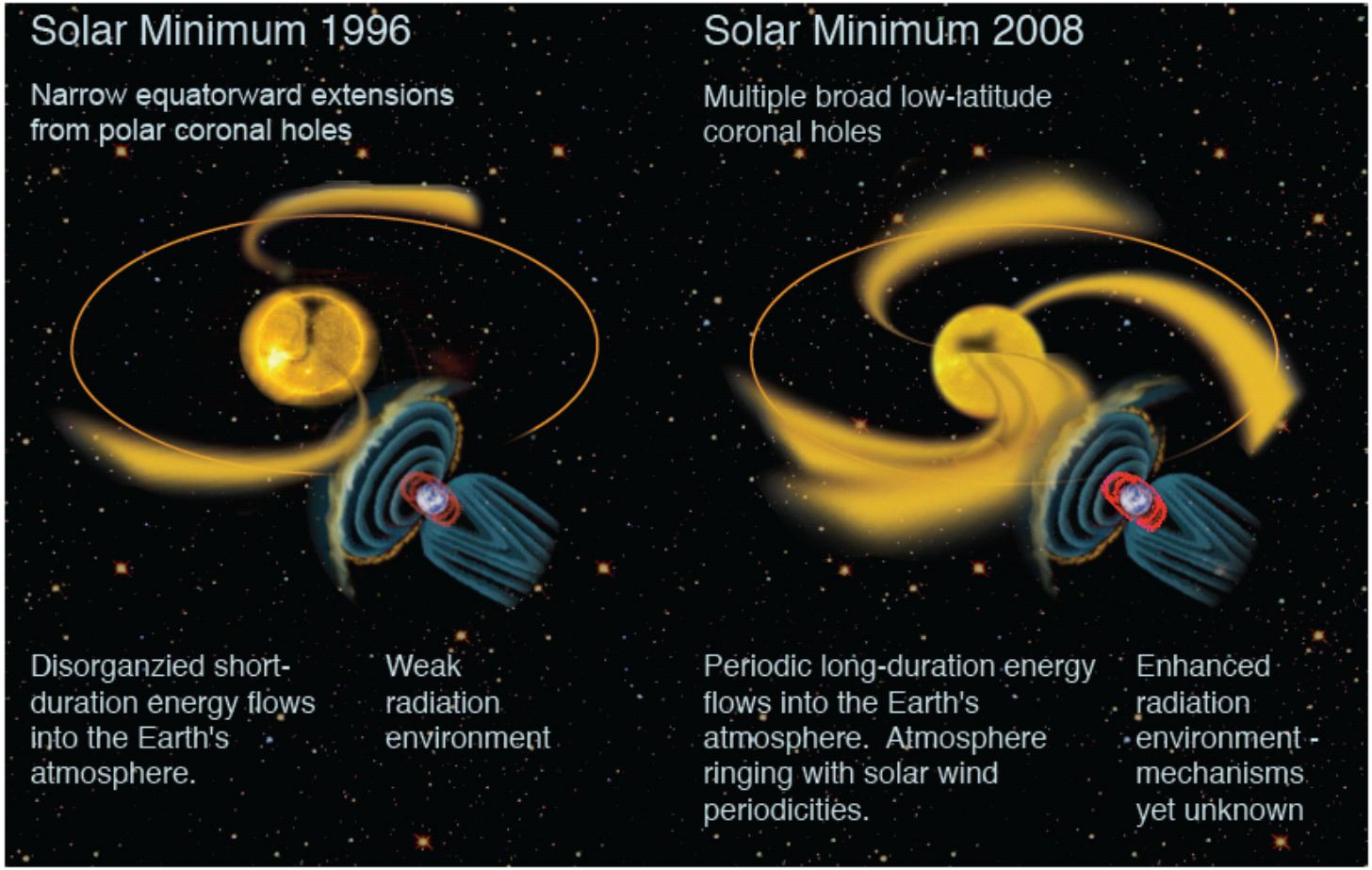
Solar Minimum 1996
Narrow equatorward extensions from polar coronal holes
Disorganzied short-duration energy flows into the Earth's atmosphere.
Weak radiation environment
Solar Minimum 2008
Multiple broad low-latitude coronal holes
Periodic long-duration energy flows into the Earth's atmosphere. Atmosphere ringing with solar wind periodicities.
Enhanced radiation environment - mechanisms yet unknown

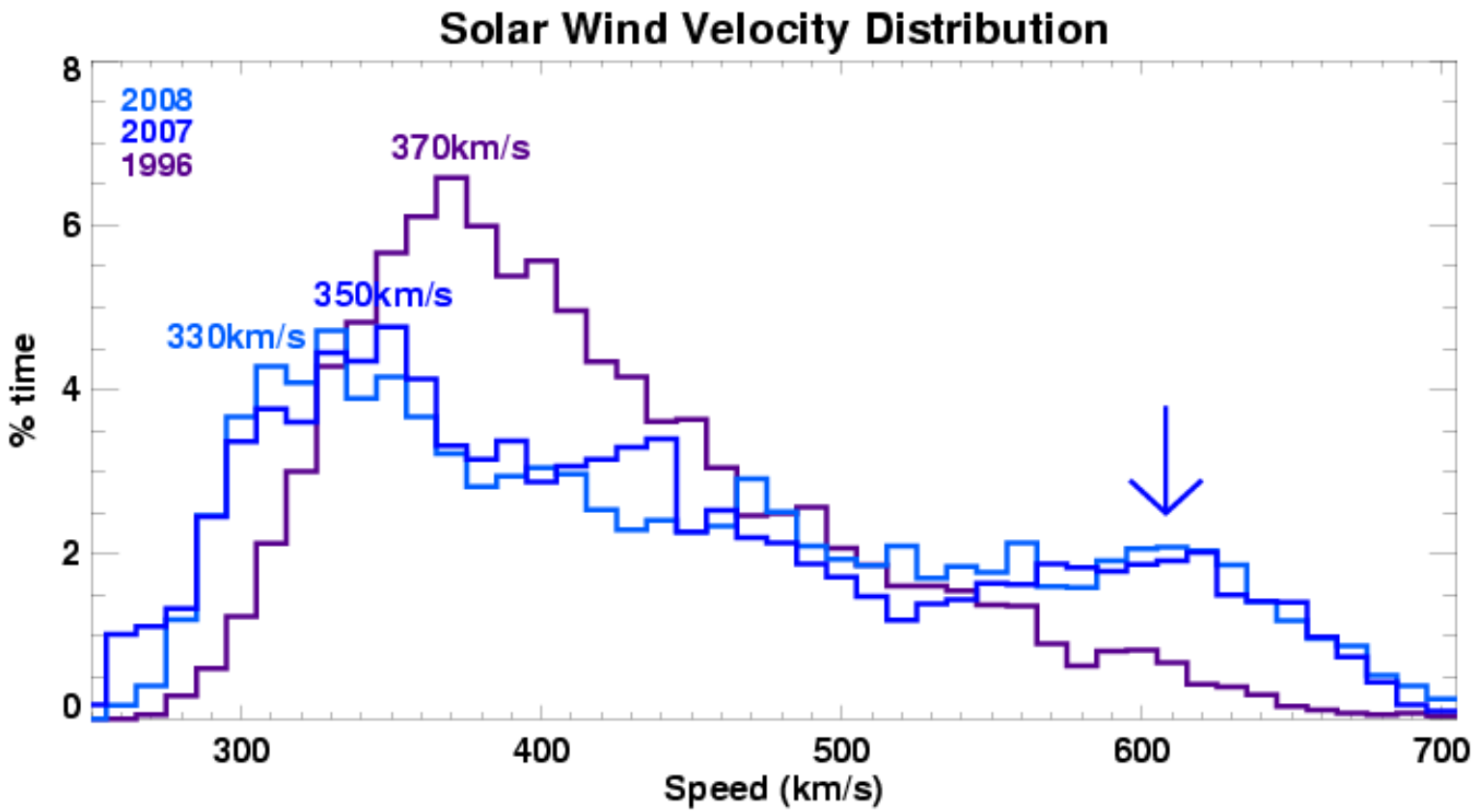
Solar Wind Velocity Distribution
2008
2007
1996
370km/s
350km/s
330km/s
% time
Speed (km/s)
0
2
4
6
8
300
400
500
600
700

WSM in 9 Carrington Rotations

9 13.5 27 sa

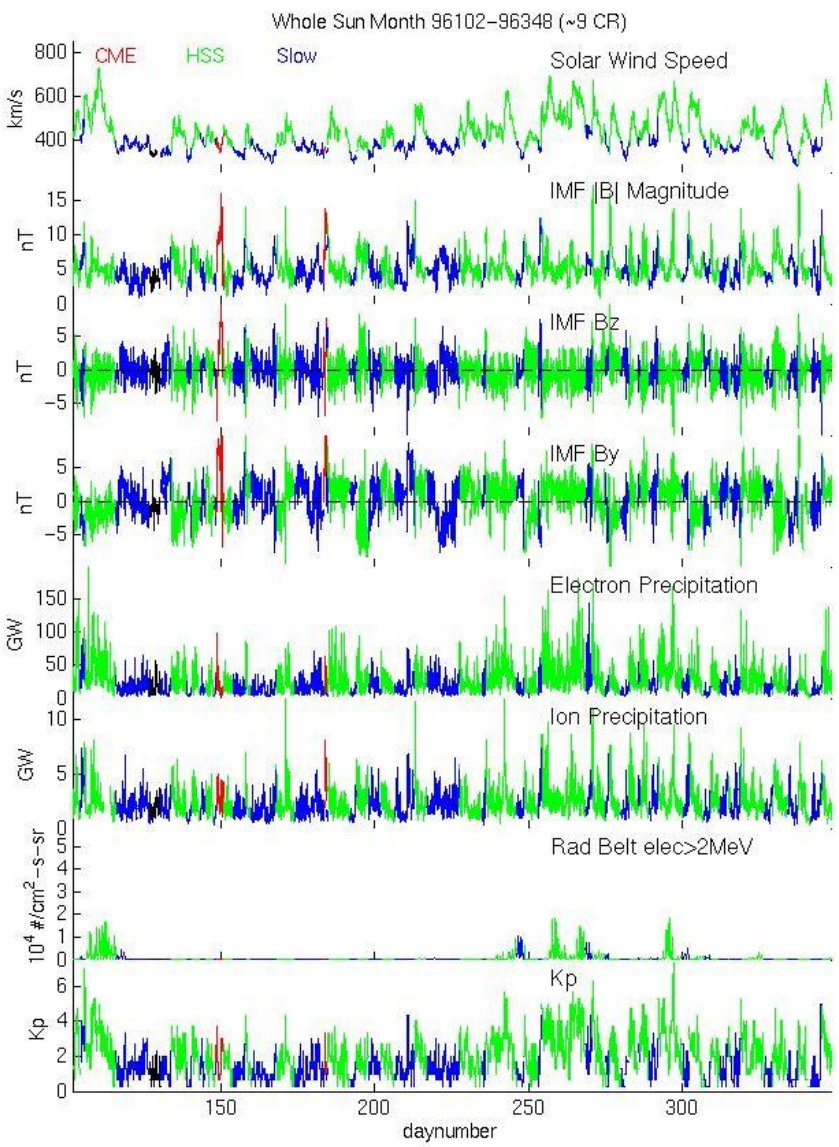

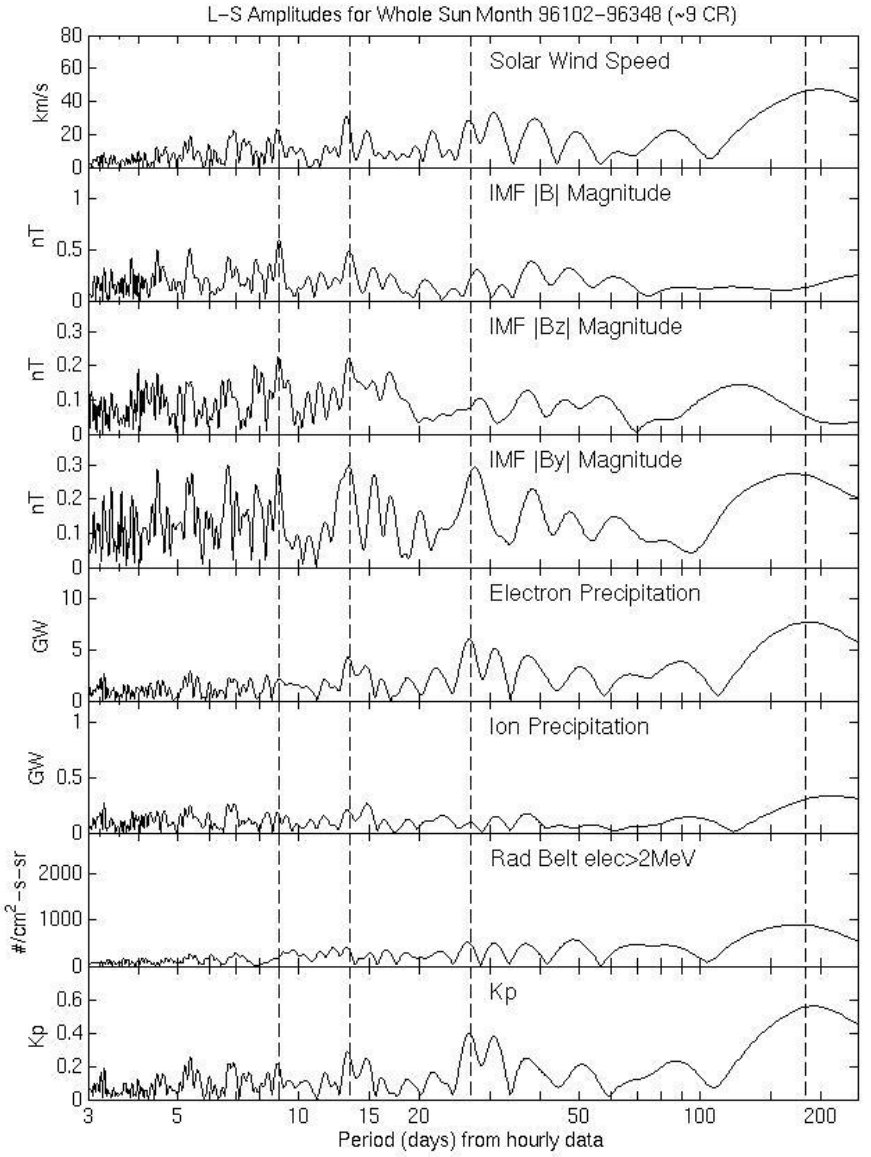

WHI in 9 Carrington Rotations

9 13.5 27 sa

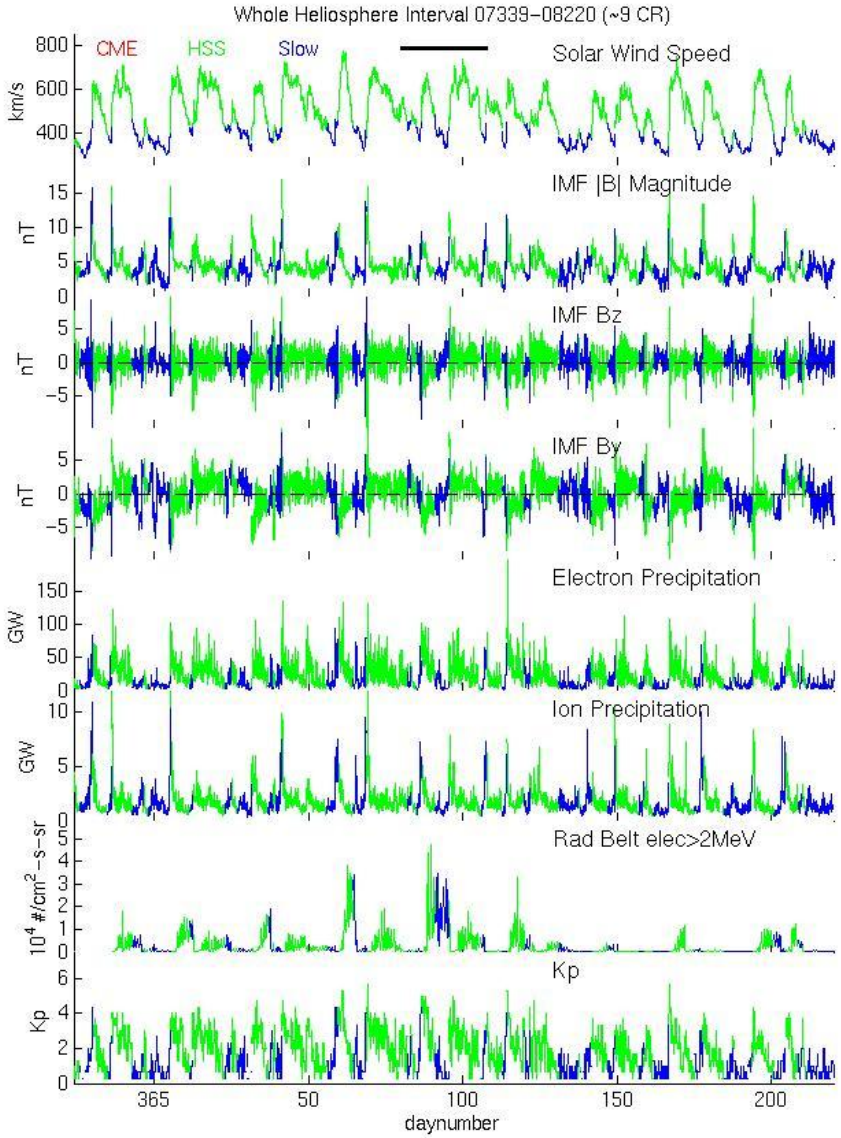

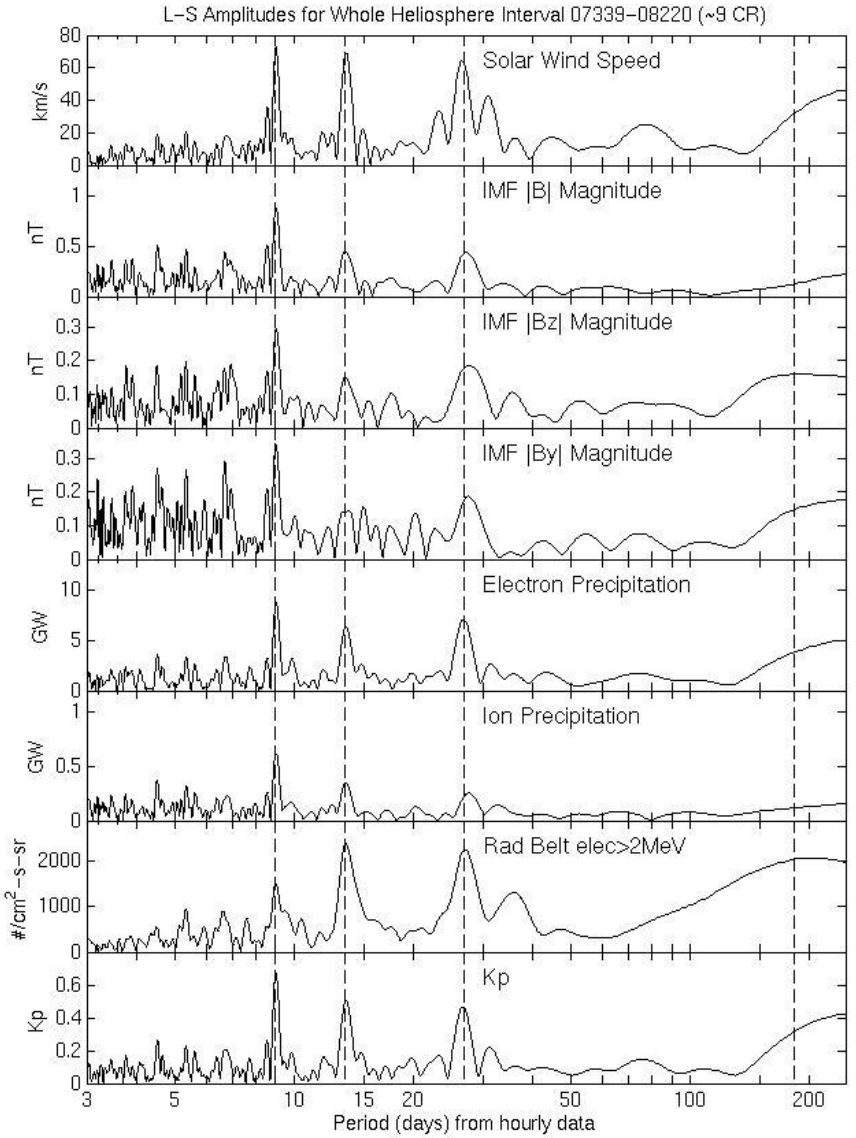

Wavelet Analyses

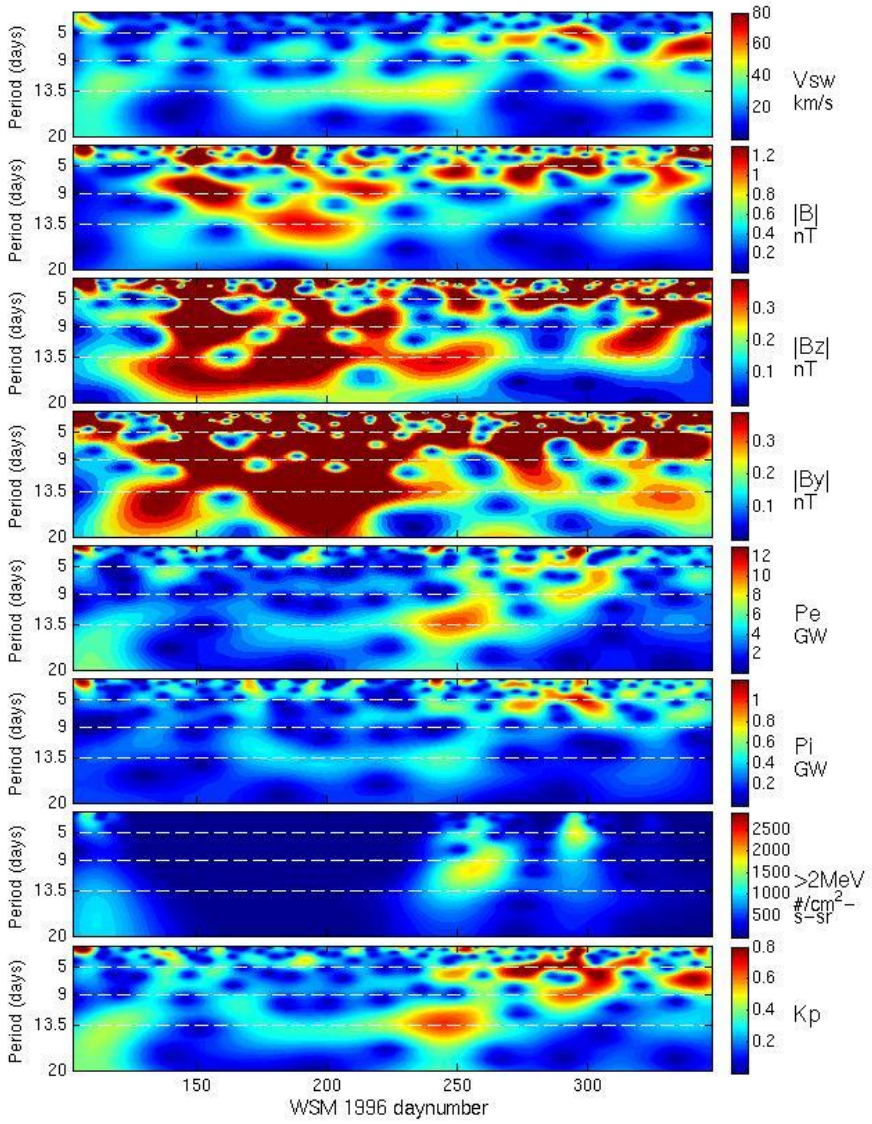

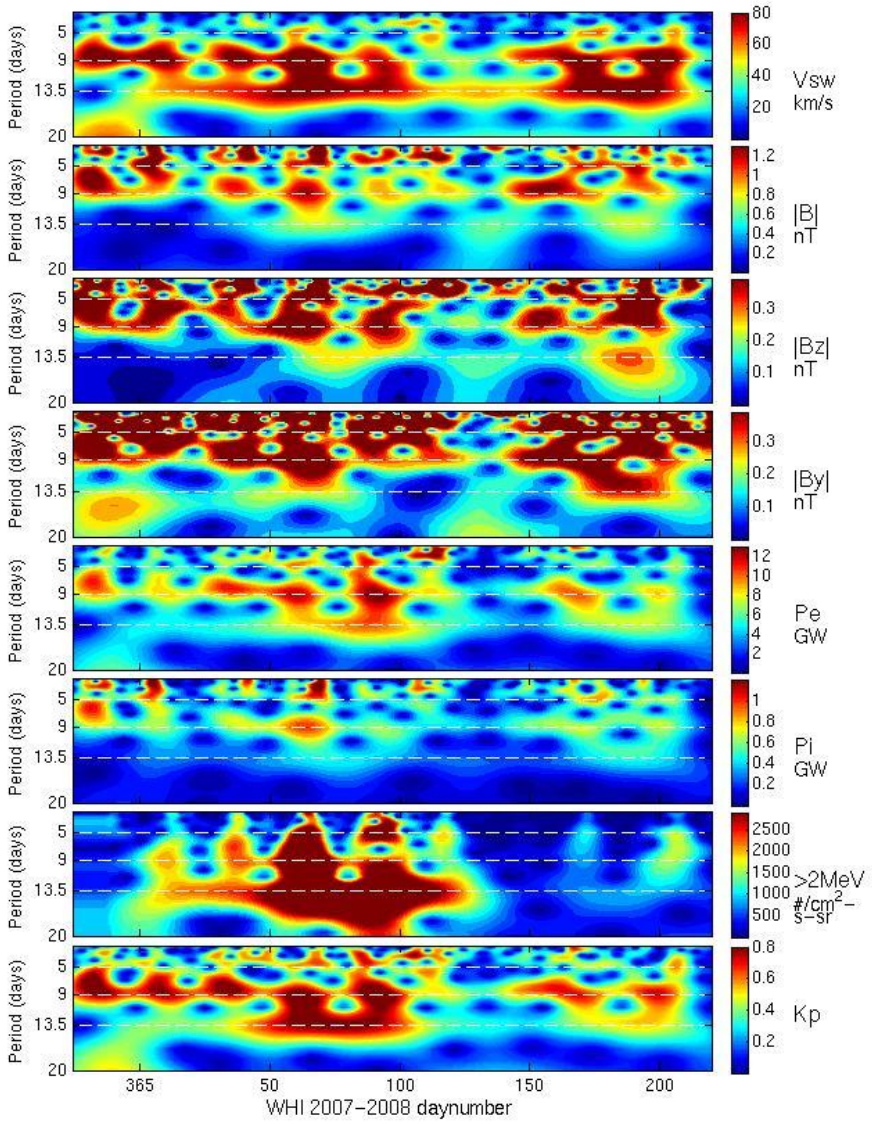

Wavelet analysis

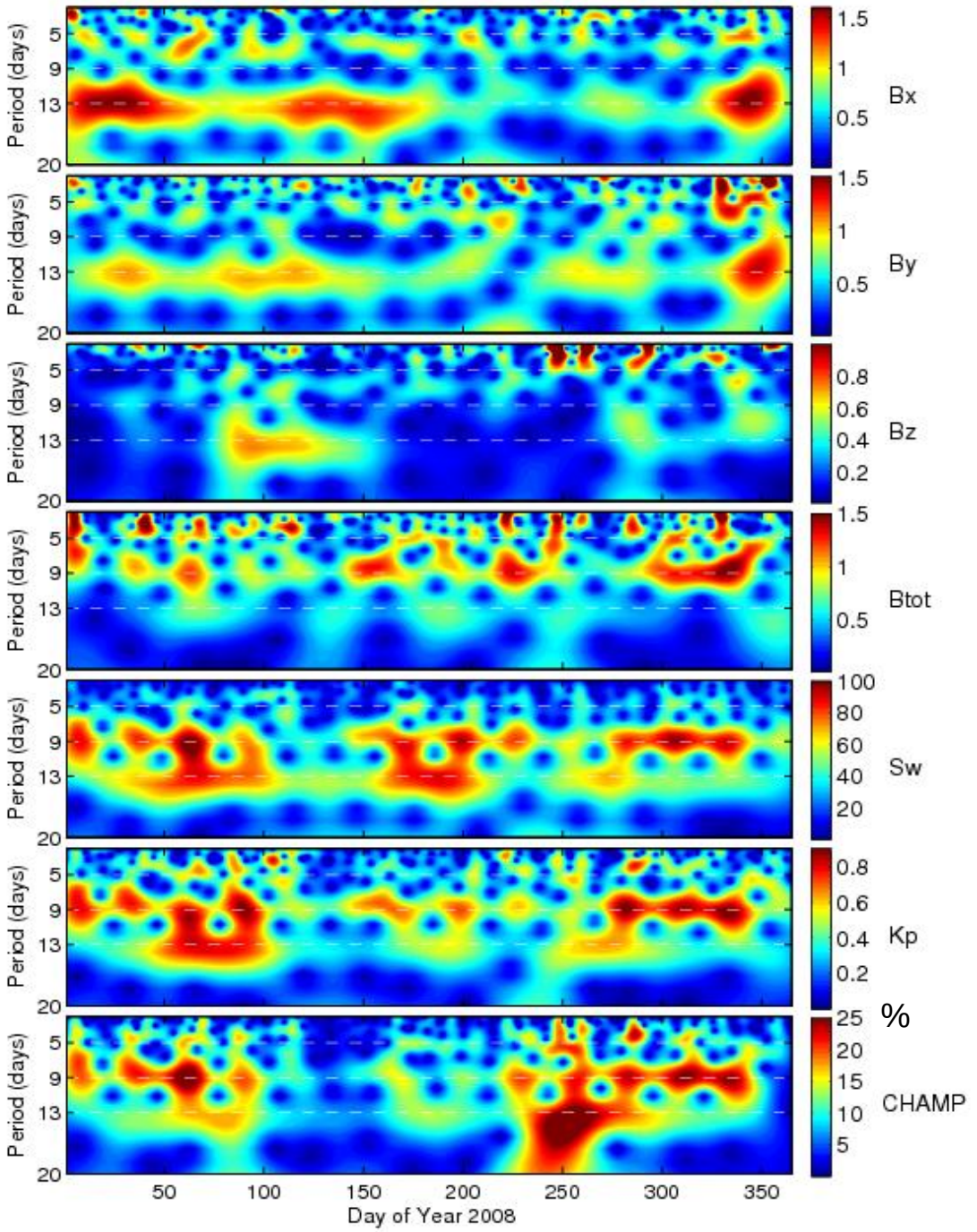

Solar Minima are Similar

- Whole Sun Month (96223-96252)
  - Monthly SS#=0.9
  - 4% CME, 47% HSS, 49% slow speed wind
  - Pe ~23.3 GW
- Whole Heliospheric Interval (08080-08107)
  - monthly SS#=0.5
  - 4% CME, 46% HSS, 50% slow speed wind
  - Pe ~22.1 GW (-5%)

Solar Minima are Different

- SC 22-23
  - Strong dipole solar magnetic field
  - Big Coronal Holes, weak low-latitude extensions
  - Vsw periodicities: 27, 13, 9-d ~45, 21, 16 km/s
  - IMF B ~4.7nT; Vsw ~415 km/s; Dsw ~8 #/cm^3
  - Outer radiation belt depressed in magnitude
- SC 23-24
  - Weaker dipolar solar magnetic field (-35% polar magnetic flux)
  - Small Coronal Holes, large low-latitude extensions
  - Vsw bimodal with periodicities: 27, 13, 9-d ~51, 45 (x2), 48 (x3) km/s
  - IMF B ~4.0nT (-15%); Vsw ~448 km/s (+8%); Dsw ~5 #/cm^3(-35%)
  - Outer radiation belt pumped up (~3.4x, +75% log)

Solar Forcing

- Transients contribute ~40% and ~6% to Pe in solar maximum and minimum, respectively. Transients represent the largest |B| values, and are more effective in producing Pe during Bz negative conditions, and less effective in producing Pe during Bz positive conditions than HSS and slow-speed wind.
- HSS contribute ~57% and ~32% to Pe in descending and solar maximum phases. HSS determine the structure of the total Vsw or Pe, and contribute the most to periodicities.
- Solar minima in 1996 and 2008 are different in solar magnetic fields, coronal hole distributions, Vsw distributions and periodicities, and solar wind densities which lead to profound effects in the Earth's radiation belts, aurora, magnetic activity, and upper atmosphere.
- The 'semi-annual' amplitudes from Lomb analyses were large ~1995-1999 for Vsw and Pe. In ~1996 (WSM), the Vsw 'sa' periods peaked in the equinoxes, enhancing the 'normal' equinoctial peaks in Pe from Russell-McPherron mechanisms, etc. The semi-annual amplitudes were absent or weak ~2002-2008 (WHI).
- The 9-day periodicities in Vsw (especially in HSS), Pe and Pi seen after 2003 were strong in 2005 and 2008 (WHI), and were absent or weak ~1997-2002 (WSM). They are also present in Kp, the neutral thermosphere density in WHI, TEC (Lei et al., GRL, 2008), and infrared [NO] and [CO2] cooling (Mlynczak et al., GRL, 2008), and are absent or weak in SEE flux, and 10.7 cm solar flux (Lei et al., JGR, 2008) . 9-day periods also in 1976 and 1983.

References

- Emery et al. (2008), Seasonal, Kp, solar wind, and solar flux variations in long-term single-pass satellite estimates of electron and ion aurora hemispheric power, J. Geophys. Res., 113, A06311, doi:10.1029/2007JA012866.
- Emery, Richardson, Evans, and Rich (2009), Solar wind structure sources and periodicities of auroral electron power over three solar cycles, J. Atmos. Terr. Phys., HSS Special Issue, doi:10.1016/j.jastp.2008.08.005.
- Gibson, S. E., Kozyra, J. U., de Toma, G., Emery, B. A., Onsager, T., Thompson, B. J., 2009, If the sun is so quiet, why is the Earth ringing? A comparison of two solar minimum intervals. J. Geophys. Res., accepted June 2009.
- Lei, J., Thayer, J. P. Forbes, J. M., Sutton, E. K., Nerem, R. S., Temmer, M., Veronig, A. M., 2008, Global thermospheric density variations caused by high-speed solar wind streams during the declining phase of solar cycle 23. J. Geophys. Res., 113, A11303, doi:10.1029/2008JA013433.